Environmental Research 310 (2026) 126023



Contents lists available at ScienceDirect

Environmental Research

journal homepage: www.elsevier.com/locate/envres





Pulmonary toxicity of particulate-phase combustion byproducts from lithium-ion battery fires

Adam Nored [a], Gavin P. Horn [b], Richard M. Kesler [b], Adam Barowy [b], Alex Schraiber [c], Benjamin Gaudet [c], Alexander C. Mayer [d], Kenneth W. Fent [d], Micah Niemeier-Walsh [d], David Naiman [e], Logan M. Klein [e], Mette Schladweiler [a], Wanda Williams [a], Rachel Grindstaff [a], Kasey Kovalcik [a], Joseph Patrick Pancras [a], Andrew F.M. Johnstone [a], Julia E. Rager [f], Stephen H. Gavett [a], M. Ian Gilmour [a], Yong Ho Kim [a,*]

[a] Center for Public Health and Environmental Assessment, United States Environmental Protection Agency, Research Triangle Park, NC, USA
[b] Fire Safety Research Institute, UL Research Institutes Columbia, MD, USA
[c] UL Solutions, Northbrook, IL, USA
[d] National Institute for Occupational Safety and Health, Cincinnati, OH, USA
[e] ORISE, United States Environmental Protection Agency, Research Triangle Park, NC, USA
[f] Department of Environmental Sciences and Engineering, Gillings School of Global Public Health, University of North Carolina, Chapel Hill, NC, USA

ARTICLE INFO

Keywords:
Lithium-ion batteries
Combustion
Metals
Bioinformatics
Pulmonary toxicology

ABSTRACT

The frequency of lithium-ion battery (LIB) fires is increasing globally, creating new challenges for firefighters and growing public safety concerns from smoke and intense heat. However, the health effects from exposure to LIB fires are not well understood. We collected soot and smoke particulate matter (PM) from LIB thermal runaway events (10 and 2 fire tests for soot and PM samples, respectively), filtered them to remove non-inhalable particles (>10 μm), analyzed for chemical composition and assessed for lung toxicity and pulmonary function in mice at 4 h and 24 h post exposure to 100 μg of the sample. Chemical and biological results were analyzed using a computational approach to identify hazardous chemical components that were potentially responsible for toxicity outcomes. Computational findings were further compared to those produced by other sources of air pollution. The soot sample contained more carbon species than the smoke PM sample (37% vs. 18%), whereas anions were higher in the PM sample (12% vs. 6%), and concentrations of inorganic elements were similar (23% vs. 28%). Fluoride particulate was found to account for up to 5% of the mass of each sample. Only soot significantly increased ventilatory timing and peak expiratory flow in mice and decreased relaxation time, while both samples caused significant increases in inflammatory responses. Soot and PM exhibited similar lung inflammatory outcomes relative to those caused by previously reported combustion-related air pollution sources. Computational analysis indicated that fluoride, Al, Fe, Ni, and Li from both samples were significantly associated with the lung toxicity responses ($p < 0.05$). The findings indicate that LIB fire soot and PM that contain hazardous metals and fluoride elicit pulmonary toxicity responses comparable to other sources of air pollution, increasing the need for awareness of potential strategies to mitigate public health impacts.

1. Introduction

Lithium-ion battery (LIB) applications are present in many of today's products including consumer electronics, mobility devices, and electric vehicles (EVs). The number of electrically powered micromobility products such as scooters, bicycles, and motorcycles, as well as their charging and usage infrastructure, are increasing in major cities in the United States (Bharadwaj et al., 2024; US Department of Energy). This increase is reflected in the number of micromobility services and recorded trips, not including unregulated and untracked devices (NACTO, 2023). Similarly, the number of EVs on the road is growing quickly. In 2012 there were less than 200,000 EVs on the road. By 2020 that number had grown to over 10 million. Today, there are over 40 million EVs in use around the world (Bharadwaj et al., 2024). LIBs are

* Corresponding author.
E-mail address: kim.yongho@epa.gov (Y.H. Kim).

https://doi.org/10.1016/j.envres.2026.126023
Received 5 August 2026; Received in revised form 1 October 2026; Accepted 26 October 2026
Available online 28 October 2026
0013-9351/Published by Elsevier Inc. This is an open access article under the CC BY-NC license (http://creativecommons.org/licenses/by-nc/4.0/).

the dominant battery technology for powering these products. The benefits for using LIBs in the product design compared to other battery or energy (i.e., combustion) technologies include a long lifespan, high energy and power density, no memory effects, and low environmental emissions (Tran et al., 2022).

With the increasing numbers of LIB powered products comes the increased risk of thermal runaway events and LIB fires (Bugryniec et al., 2024). According to a report by the National Fire Protection Association (NFPA), citing LIB fires in New York City, there was an increase from 30 LIB-related incidents in 2019 to 279 incidents in 2024 (Roman, 2025). This represents an increase of more than nine-fold in five years with estimated costs from these events totaling more than $500 million (UL White Paper, 2025). Most fires involving LIBs are caused by thermal runaway events (Sun et al., 2021). Because LIBs are often concealed within the geometry of a product, fire suppression and cooling are challenging. In some cases, LIB fires have been known to reignite, sometimes several hours or days after the initial thermal runaway event (Hynynen et al., 2023; Sun et al., 2021). LIBs may enter thermal runaway from internal short circuits caused by defects in the battery cells or from damaged or misused (overheated, punctured, crushed, overcharged) battery cells (Wang et al., 2019). Thermal runaway is characterized by the cell temperature increasing in an uncontrollable and irreversible fashion due to exothermic reactions inside the cell (Bugryniec et al., 2024; Tran et al., 2022). The increased energy density of LIBs also decreases their thermal stability (Feng et al., 2018). Propagation of thermal runaway is also possible, especially in tightly packed cells due to heat transfer from the high temperature cells and flames.

LIB fires emit a mixture of gases and particulate matter (PM) in smoke that may be toxic to people and the environment. Individuals near LIB smoke emission sources can inhale the smoke PM generated by the fire; and depending on smoke dispersion patterns, these exposures can also impact individuals that are further away. Recent studies into the components of smoke and PM generated in LIB fires have identified several hazardous combustion chemicals including hydrogen fluoride (HF), hydrogen cyanide (HCN), hydrochloric acid (HCl), polycyclic aromatic hydrocarbons (PAHs) and heavy metals (Hynynen et al., 2023; Kwon et al., 2024; Said et al., 2019; Sturm et al., 2022; Sun et al., 2021; Zhang et al., 2019). After the fire has been extinguished, there are other hazards. Soot from the fire can contain toxic elements that persist in the environment, posing risks during the post-fire investigation process and cleanup process. Individuals may be exposed to soot dermally or by inhaling re-aerosolized PM when the remains of the fire are disturbed, as well as during property restoration. There have been multiple studies into the gases emitted during a LIB fire; however, the PM composition of the smoke has largely been understudied with only a few articles recently being published on this topic (Claassen et al., 2024b; Adanouj et al., 2023; Premnath et al., 2025).

Residue and soot samples from LIB fires have been determined to contain semi-volatile organic compounds (SVOCs) (Palma et al., 2024) and transition metals (Fe, Li, Co, Ni, and Mn) that are key components of the battery system (Sturm et al., 2022). Characterization studies conducted on emissions from LIB fires (Claassen et al., 2024b; Adanouj et al., 2023; Premnath et al., 2025) have also found the same metals, phosphates, ionic compounds, organic carbon (OC) and elemental carbon (EC). There were up to 30 different elements found with particles identified in the inhalable size range in the PM studies. There is a gap in our understanding of what could be toxic in the elemental, OC, EC and ionic makeup of inhalable particles in combustion byproducts from LIB fires. Continuing these PM characterization studies and adding a toxic response focus area will help increase our understanding of possible dangers inherent to LIB fires.

This study was conducted to increase the knowledge of different components in the particulate-phase combustion byproducts (smoke PM and soot) created during LIB fires and their lung toxicity responses following acute exposures in mice. Findings of this study were further compared to our previous findings from urban air pollution and various combustion smoke exposure studies, to gain insight into the unique properties of smoke particles from LIB fires, the relative potency and what individual components cause adverse effects.

2. Methods

2.1. LIB fire test and combustion sample collection

LIB fire tests were conducted at an indoor fire laboratory (UL Solutions, Northbrook, IL). Fig. 1 shows an experimental setup and combustion byproducts after the LIB fire tests. The test utilized 18650 cells (cylindrical NCR rechargeable cells with lithium nickel cobalt aluminum oxide (NCA) chemistry) with 3300 – 3400 mAh capacity at 100 percent stage of charge. Twenty-five cells were placed in a 5 × 5 array inside a 100 mm × 100 mm enclosure were driven to thermal runaway by heating two central cells with a 24 V flexible film heater at 4 – 7°C per minute (UL 2596, 2023). The resulting thermal runaway propagated to the remaining 24 cells of the test setup. The test captured emissions from the container with a vent opening, which is representative of a real-world situation, such as a power-tool battery or external battery pack overheating, entering thermal runaway, melting the enclosure, and ejecting smoke and PM. Airborne whole smoke PM was collected on 90 mm glass fiber filters using high volume samplers (Staplex, Cincinnati, OH) during 2 consecutive LIB fire tests over a period of 187 min. The sampler was operated at a flow rate of approximately 280 L/min. Soot was collected from 10 different fire tests. The soot was collected onto clean paper, weighed, and transferred to sample vials after the fire had been allowed to burn completely. The PM was extracted from the filters through sonication in a HPLC-grade methanol. The sample was then dried and weighed. For chemical analysis, samples of both soot and PM were separately resuspended in a HPLC-grade methanol solution and filtered (Syringe Strainer, pluriSelect, El Cajon, CA) to remove non-inhalable particles above 10 μm. Note that the filtered particles may not be directly related to an aerodynamically defined PM10 (particles with an aerodynamic diameter of 10 μm or smaller) but since combustion particles generally have a density greater than 1 g/cm^3 (Ouf et al., 2019), their physical diameters will be smaller than their aerodynamic diameters, suggesting that the filtered particles in this study won't be larger than PM10. The samples were diluted to a concentration of 1 mg/mL. Three aliquots of each sample containing 200 μg of PM or soot were added to pre-cleaned 15 mL polypropylene DigiTubes (SCP Science, Quebec, Canada) and submitted for chemical analyses such as organic carbon (OC), elemental carbon (EC), inorganic elements and ions analyses. Due to shortage of the samples available, physical characteristics of the particles such as morphology, particle size distribution, and agglomeration, were not determined. For toxicity testing, separate samples of soot and PM were suspended in a saline solution at a concentration of 2 mg/mL.

2.2. LIB combustion sample analysis

For the inorganic elemental analysis, an aliquot of 0.5 mL of inverse aqua regia, composed of three parts nitric acid and one-part hydrochloric acid (Fisher Scientific, Fair Lawn, NJ), was added to each sample tube. The DigiTubes were then heated in a DigiPrep Jr heating block system (SCP Science) at 65°C for 2 h. Following this step, the tubes were withdrawn, 0.5 mL of deionized water was added, and they were returned to the DigiPrep Jr and heated at 95°C for an additional 2 h. The resulting solution was allowed to leach overnight. The following day, 9 mL of deionized water was added to each DigiTube, and the contents were vortex-mixed and then centrifuged at 2000 rpm for 30 min. An aliquot of the supernatant was subsequently transferred for elemental analysis, following further dilution to achieve a final nitric acid concentration of 2%. Inorganic elemental analyses were performed in duplicate and using high resolution inductively coupled mass spectrometry (HR-ICP-MS; Nu AttoM ES; Nu Instruments Ltd, Wrexham,

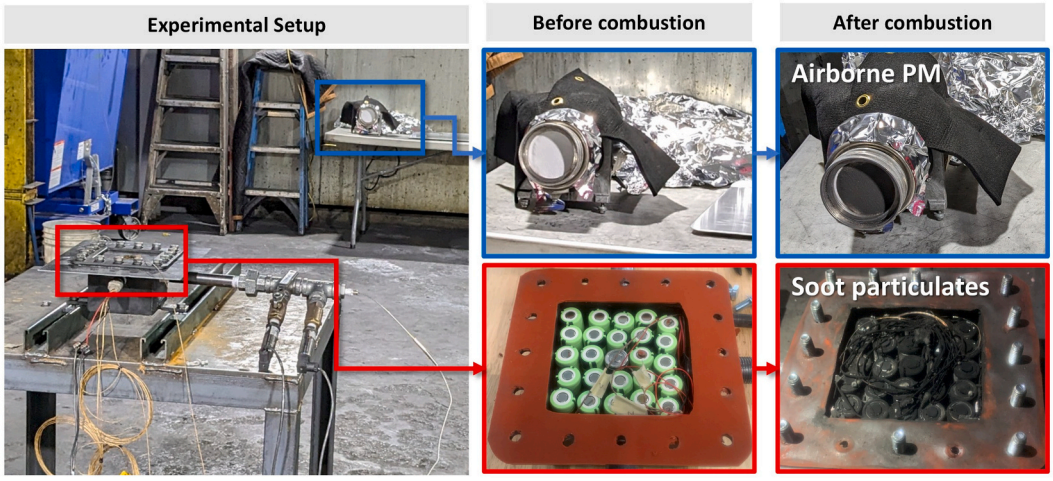


Fig. 1. Before and after of a thermal runaway of Li-ion battery (LIB) cells with emissions capturing systems present.

UK). Samples were introduced to the plasma using a SC-FAST flow injection multivalve system and MC2 peristaltic pump (Elemental Scientific Inc., Omaha, NE) with on-line internal standard Indium at 2 ppb. Up to forty-two elemental isotopes were analyzed, including typical metals found in LIBs such as Al, Co, Li, Mn, Ni, Pb, Sb. Analytical calibration was performed using multielement standards (SCP Science). NIST SRM 1643a and 1640a were analyzed in each analytical sequence as a quality control measure. For water soluble anion analysis, samples were diluted to 5 mL using Milli-Q water (Millipore Sigma, MA) prior to transfer into Thermo Scientific Dionex vials and Guardcaps. Ion Chromatography analysis was performed on a Dionex ICS-2000 (Chromeleon software v6.8) equipped with a 200 µL injection loop, Thermo Scientific Dionex IonPac AS18 anion-exchange analytical (4 × 250 mm, pn060549) and AG18 guard columns (4 × 50 mm, pn060551) utilizing a 30 mM potassium hydroxide isocratic separation method, based on EPA Method 300.0(A). The system was calibrated using a Thermo Seven Anion standard (pn056933) of fluoride, chloride, nitrite, bromide, sulfate, nitrate and phosphate. Each sample was injected and analyzed twice to observe precision. For carbon species analysis, samples were analyzed using a Sunset Laboratory Model 5 L Thermal-Optical Carbon Analyzer (Sunset Laboratory Inc., Tigard, OR). In preparation for analysis, each sample solution was homogenized using a vortex mixer for 1 min. An aliquot of 20 µL was extracted from the well-mixed solution using a syringe and directly spiked onto the center of a pre-baked quartz filter punch. The spiked filter punch was dried using the equipment's drying cycle function to ensure methanol evaporation. Once dried, the OC/EC analysis was conducted in triplicate and using NIOSH 870 parameters (NIOSH Method 5040). The resulting organic carbon, elemental carbon, and total carbon values were recorded.

2.3. Experimental animals

Adult pathogen-free female CD-1 mice (8–10-week-old) were purchased from Charles River Breeding laboratories (Raleigh, NC) and housed for a minimum of five days before start of study. Animals were kept in the EPA animal facility (accredited by the Association for Assessment and Accreditation of Laboratory Animal Care) and fed rodent chow and water ad libitum. Mice were weight-randomized into groups of 6 for each exposure condition. Mice with extremely high and low baseline weights were excluded after randomization. Mice were treated humanely regarding alleviation of suffering. After exposure to combustion samples, animals were euthanized by intraperitoneal injection of sodium pentobarbital and phenytoin sodium (Euthasol; Virbac AH Inc., Fort Worth, TX).

2.4. Exposure to LIB combustion samples

Prior to exposures, mice (n = 40) were anesthetized using a vaporized isoflurane (Abbott Laboratories, Green Oaks, IL) technique discussed previously (Kim et al., 2021). Mice were dosed with 100 µg of a combustion sample via oropharyngeal aspiration. PM and soot samples were separately administered and were assessed at 4 h and 24 h after exposure (24 mice for 2 exposure conditions at 2 time points). Separate groups of mice were used for control, with the negative control group being instilled with 50 µL of saline (12 mice at 2 time points) and the positive control group (4 mice at 2 time points), used to confirm the mice could respond to an inflammatory stimulus, was instilled with a solution of 2 µg of lipopolysaccharide (LPS) in 50 µg of saline (lipopolysaccharides from *Escherichia coli* O111:B4, Sigma, St. Louis, MO). The selection of the dose (100 µg) was based on extreme exposure levels (>1000 µg/m^3) of particles from LIB fires (Jo et al., 2024; Meister et al., 2025). If exposures are near or close to the fires (assuming >3000 µg/m^3 of particles), particles deposited in the human lungs for 24 h would be 123 ng/cm^2 (Kim et al., 2018). In the present study, the dose (100 µg) to the mouse lung was calculated to be 126 ng/cm^2, assuming the respiratory deposition fraction by the oropharyngeal aspiration method and surface area of 0.81 and 642 cm^2, respectively (Foster et al., 2001; Weibel, 1973), and appeared to be relevant to the inhaled smoke particle concentrations in human lungs (123 ng/cm^2).

2.5. Breathing parameter assessment

Pulmonary function that can be evaluated by ventilatory parameters was determined before exposure (baseline) and approximately at 4 h and 24 h after exposure, using a whole-body plethysmography (WBP) system (Emka Technologies, Falls Church, VA) as previously described (Kim et al., 2021). In this system the mouse had complete freedom of movement in a small clear plastic chamber (3.5″ diameter x 2.5” height). Mice were given marks on the tail to identify individuals within each cage prior to the acclimation in the chamber. Mice were acclimated for approximately 20 min before the exposure day. The WBP chambers were calibrated by injecting a predefined volume of air using a 20 mL syringe. The IOX software (Emka Technologies, Falls Church, VA) established the pressure-volume relationship that was used to extrapolate changes in chamber pressure to changes in chamber volume associated with breathing patterns in mice. On the exposure day, mice were placed in the WBP chamber. Real-time respiratory and breathing parameters were collected and analyzed by the IOX software. The test took approximately 20 min. The parameters assessed were tidal volume (TV), breathing frequency (F), inspiratory and expiratory time (Ti/Te), peak inspiratory

and expiratory flow (PIF/PEF), minute ventilation (MV), flow at mid-tidal expiratory volume (EF50) and relaxation time (RT). In addition, time and flow rate parameters were used to evaluate an index of ventilatory timing (enhanced pause; Penh) which has previously been found to correlate with changes in breathing patterns in response to airway inflammation (Lundblad et al., 2002; Lundblad, 2012; Mitzner and Tankersley, 1998).

2.6. Lung toxicity assay

Mice were euthanized at 4 h and 24 h after exposure. Blood was collected via cardiac puncture, using a syringe primed with ethylenediaminetetraacetic acid (EDTA). White blood cell count, red blood cell count, hemoglobin, hematocrit, mean corpuscular volume, mean corpuscular hemoglobin, red cell distribution width, platelet count, plateletcrit, mean platelet volume, neutrophils, and lymphocytes were measured using a Hemavet 950 FS Hematology Analyzer (Drew Scientific, Inc., Miami, FL). Bronchoalveolar lavage fluid (BALF) was collected from the right lung lobes and used to determine the total cell count and differential analysis of macrophage and neutrophil numbers. Total BALF cell count of each mouse was determined using a Coulter counter (Coulter Co., Miami, FL). BALF supernatants were examined for protein content, albumin, N-acetyl glucosaminidase (NAG), γ-glutamyl transferase (GGT), and lactate dehydrogenase (LDH). Albumin and protein content was determined using the SPQ test system (DiaSorin, Stillwater, MN) and the Coomassie plus protein assay (Pierce Chemical, Rockford, IL), respectively. NAG was determined using a NAG assay kit (Roche Applied Science, Indianapolis, IN), as well as GGT and LDH (Gamma GT Reagent and LDH-L Reagent, Thermo Scientific, Middletown, VA). Cytokines tumor necrosis factor-α (TNF-α), interleukin-6 (IL-6), and macrophage inhibitory protein-2 (MIP-2) in BALF supernatants were determined using multiplexed fluorescent bead-based immunoassays (Milliplex xMap Kit, MilliporeSigma, Burlington, MA) and read with a FLEXMAP 3D (Luminex Co., Austin, TX). All values below the limits of detection (LOD) were imputed at one half of the LOD.

2.7. Statistical analysis

Biological (inflammatory and injury biomarkers) and physiological (breathing parameters) data were analyzed using one-way analysis of variance (ANOVA) followed by Dunnett's multiple comparison test. An unpaired *t*-test (two tailed) was also performed to determine whether significant differences existed between two exposure groups (soot vs. smoke PM). Statistical analysis was done in GraphPad Prism (version 6.0, GraphPad Software Inc., San Diego, CA). Data were expressed as mean ± standard error of the mean (SEM). The statistical significance level was assigned at probability value of $p < 0.05$.

2.8. Computational network analysis

Chemical and biological analysis data were used to understand inter-chemical relationships and relationships between chemicals and biological outcomes. A weighted chemical co-expression network analysis (WCCNA) was applied to elucidate relationships in this study, alongside similar previously published chemical-outcome datasets produced by our team to more holistically support identified relationships. This analysis was performed using the weighted gene co-expression network analysis package in R (v.2025.05.0). A detailed description of the WCCNA is provided in our previous papers (Kim et al., 2022; Klein et al., 2026; Rager et al., 2021). The input matrix for this analysis is listed in Supplementary Table S1 and S2. Chemicals were analyzed in an unsupervised manner to identify the significant chemical group (module) related to biological response profiles (traits) using a data-reduction method followed by correlation analyses. Pearson correlation coefficients were calculated for all pairwise comparisons of chemicals and the resulting correlation matrix was transformed into an adjacency matrix resulting in a weighted network describing connection strengths between chemical distributions. A signed network was implemented, such that chemicals with positive correlations were grouped together. Correlation values within the adjacency matrix were raised to a power of 18 to maximize the scale-free topology model fit, as suggested. With this co-expression network was constructed that was weighted, emphasizing high correlations and deemphasizing low correlations between chemicals. Modules were then identified as groups of densely interconnected chemicals in the weighted network analysis with high topological overlap, measured using an average linkage hierarchical clustering with a dynamic tree-cutting algorithm. Altogether, resulting modules represented clusters of highly interconnected chemicals with positive or negative correlations. These defined modules were used to calculate module eigenvalues (ME), representing the first principal component of each module. To identify significant modules related to biological responses, chemical significance (CS) and module membership (MM) was evaluated. Each biological endpoint was evaluated separately in relation to individual chemicals, and resulting models were used to derive correlation matrixes. This WCCNA resulted in the derivation of MEs, representing the collective distribution of chemicals that are co-modulated in the tested samples. These MEs were correlated against the biological response data via Spearman Rank correlations using the Hmisc package in R. Eigenvalue correlations provide a broad overview of relationships and allow identification of relationship drivers of individual chemical-toxicity end point correlation values. The correlation was calculated using the 'cor' function; the p-value was calculated using the 'corPvalueStudent' function and visualized using the corrplot and heatmeply packages. To elucidate key chemical components and their biological responses, the relative abundance of chemicals in the soot and PM was further compared with various air pollution samples (oak and eucalyptus smoke, Ottawa ambient PM, residual oil fly ash, and diesel exhaust particles; Supplementary Table S1) that were reported in our previous studies (Kim et al., 2022; Klein et al., 2026). Note that in this direct cross-study comparison, biological outcomes were collected from the same animal species (CD-1 mouse) under the same exposure conditions (time and dose).

3. Results

3.1. Chemical characteristics of LIB fire smoke PM and soot

The mass fractions of the individual chemical components of the LIB smoke PM and soot are shown in Fig. 2. Carbon, both organic and elemental, made up 18.20% of the PM and 36.70% of the soot. For the soot sample (Fig. 2A), it was an even split, 18.60% being organic and 18.10% being elemental. For the PM sample (Fig. 2B), there was significantly more OC, comprising 13.20% of the total sample and 72.53% of the total carbon in the sample. EC made up 5.00% of the total smoke PM sample.

The inorganic elements accounted for 27.91% of the smoke PM and 23.12% of the soot sample composition. The smoke PM had five elements that accounted for nearly 90% of the inorganic content (>24% of the total composition): Ni (50.07%), Li (17.11%), Al (11.05%), Co (9.39%), and Fe (3.96%). There were several more elements making up another 3% of the total PM smoke sample. The soot sample similarly had four elements, Ni (57.42%), Li (13.13%), Al (12.21%), and Co (11.27%) that dominated the inorganic fraction (>94%) and made up a significant amount of the total sample (21.7%). The rest of the inorganic elements made up an additional 1.4% of the total soot sample. Both soot and smoke PM had a relatively large amount of particulate fluoride (3.56% and 4.81% of the total PM mass, respectively).

Other anions present in the PM sample were chloride (0.85%), phosphate (3.67%), sulfate (1.81%), and nitrate (0.74%). Chloride (0.30%) and phosphate (2.04%) were also present in smaller amounts in the soot sample, but sulfates and nitrates were not.

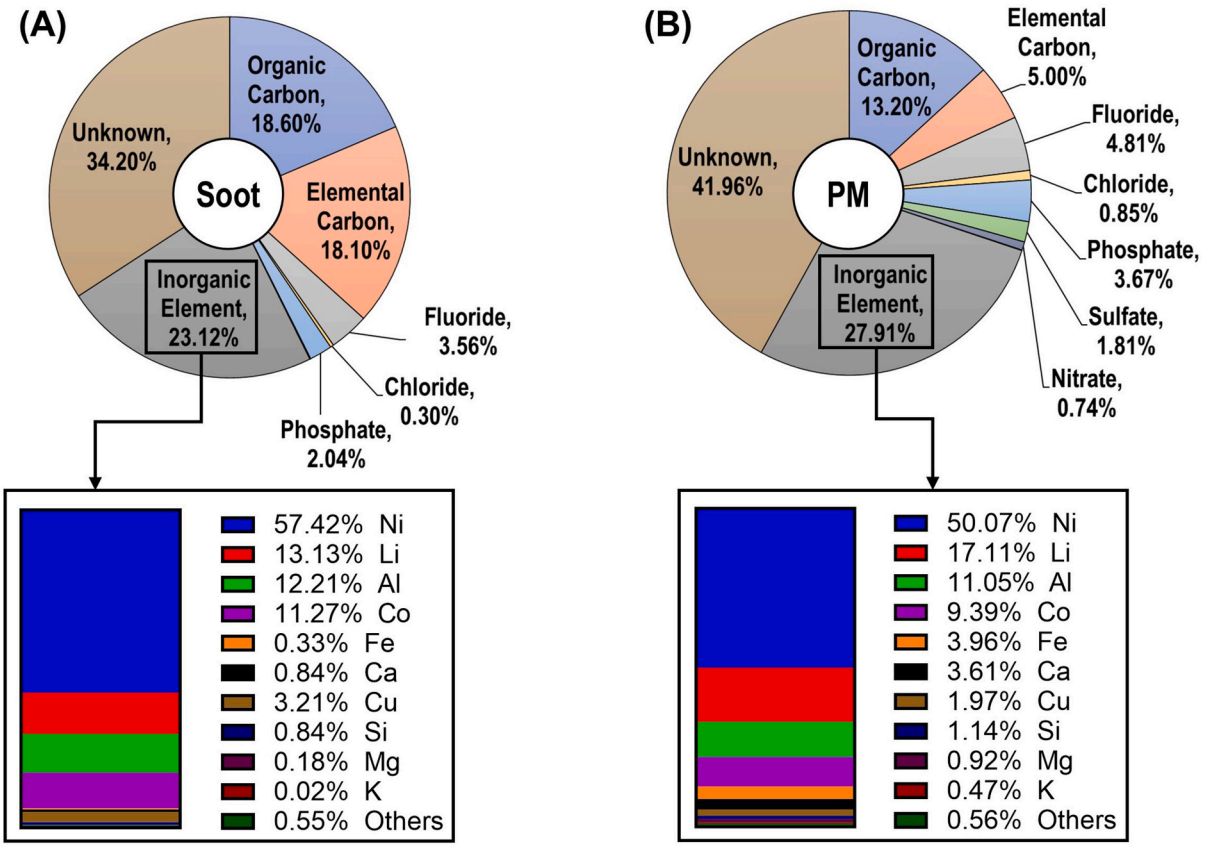


Fig. 2. Mass balance of major chemical components of combustion particulate (A) soot and (B) smoke PM from Li-ion battery (LIB) fires. Unknown: unquantified oxygen and hydrogen derivatives.

3.2. Lung toxicity

At 4 and 24 h after exposure to the combustion particles, the BALF of the mice were analyzed for neutrophil count, cellular injury biomarkers (protein, albumin, NAG, GGT, and LDH), and pro-inflammatory cytokines (TNF-α, IL-6, and MIP-2). These data are shown in Fig. 3 and Supplementary Table S3. The mice in the 24 h post exposure cohorts, exposed to either the soot or the smoke PM sample had elevated neutrophils compared to the saline control. The control cohort had less than 5×10^3 neutrophils on average, while soot and PM exposed cohorts had more than 6×10^4 neutrophils present in the lungs on average.

Protein concentration levels, a marker for vascular leakage in the lungs or pulmonary edema, also showed significant increases in the 24 h cohorts exposed to soot and PM. The control group had an average concentration less than 100 μg/mL, while the soot exposed cohort averaged 138.3 μg/mL and PM exposed cohort averaged 153.5 μg/mL. Albumin, another marker for pulmonary edema, had elevated concentrations for both the 4 h and 24 h post-exposure cohorts that were administered the PM sample. The 4 h and 24 h post-exposure groups had average concentrations of 36 μg/mL and 39 μg/mL compared to the control group's 27 μg/mL. Of the three markers that were used to analyze cellular damage (NAG, GGT, and LDH), there was little increase in the concentration of GGT in the BALF compared to the control. NAG and LDH in the exposed groups saw some increased concentrations compared to the controls, especially in the 24 h post exposure sample, but none were significantly higher.

Of the cytokines, TNF-α had no significant differences in concentrations between the cohorts administered soot or smoke PM samples and the control cohort. IL-6 and MIP-2 concentrations increased significantly for each cohort administered the soot sample. For MIP-2, both 4 h and 24 h post exposure average concentrations were significantly elevated. Concentrations were 82.65 pg/mL and 80.92 pg/mL respectively, compared to the saline control groups concentrations of 38.65 pg/mL and 40.81 pg/mL. IL-6 was similarly significantly elevated in the cohorts exposed to the soot sample, with concentrations of 87.91 pg/mL and 142.74 pg/mL for the 4 h and 24 h post exposure time points, respectively. The average saline control concentrations for those groups were 3.2 pg/mL at both time points. IL-6 was also largely (but not significantly) increased for the smoke PM sample 4 h and 24 h post-exposure cohorts with concentrations of 68.34 pg/mL and 129.69 pg/mL, respectively.

LPS data from the positive control group are not shown in Fig. 3 but listed in Supplementary Table S3. LPS exposure groups were only used to confirm that the oropharyngeal aspiration method was working properly, and mice are capable of mounting a reproducible inflammatory response in the lungs. There were no significant differences in any of the lung toxicity endpoints between the smoke PM and soot sample exposures. None of the soot or PM exposures significantly altered any of the hematological parameters studied (Supplementary Fig. S1).

3.3. Airflow and breathing parameters

WBP, the method for analysis of change to the breathing parameters in the cohort, is presented in Fig. 4 and Supplementary Table S4 and S5. There were no significant changes to the TV, F, Ti, Te, PIF, and MV parameters. A significant increase in Penh (airflow patterns in response to airway inflammation) compared to the saline control cohort was observed at the 24 h post exposure for the soot sample (0.29 vs. −0.03). The cohorts administered the soot sample also exhibited a significant difference in PEF (0.21 vs. −0.93 mL/s) and EF50 (0.03 vs. −0.71 mL/s) compared with the saline control at the 24 h time point. Compared with saline control, the soot sample decreased RT at 4 h and 24 h post

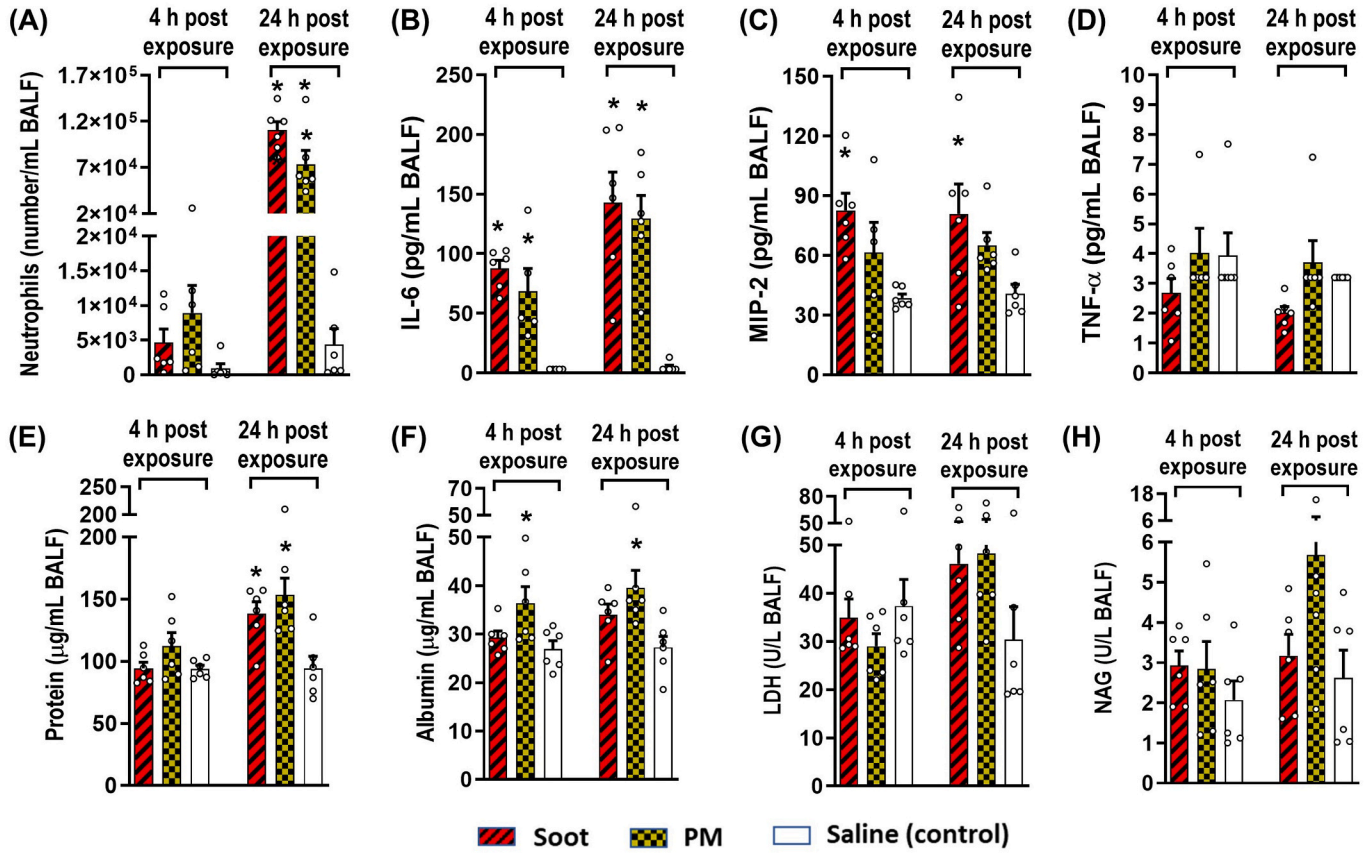


Fig. 3. Lung toxicity of mice exposed to combustion particulate (soot or smoke PM) from Li-ion battery (LIB) fires. (A) Neutrophil numbers, (B) IL-6 levels, (C) MIP-2 levels, (D) TNF-α levels, (E) Protein levels, (F) Albumin levels, (G) LDH levels, (H) NAG levels. Mice were exposed to the combustion particles (100 μg) by oropharyngeal aspiration and BALF was obtained at 4 and 24 h post exposure. Data are mean ± SEM obtained from 6 mice for each group. *$p < 0.05$ compared with saline (control) group from the same time point (one-way ANOVA with post-hoc Dunnett's test).

exposure (−6.67 vs. 14.67 ms and −8.00 vs. 17.33 ms, respectively). The smoke PM exposed group did not alter any of the breathing parameters studied. Small changes in the breathing parameters were observed between the smoke PM and soot exposed groups, but they were not significantly different.

3.4. Computational analysis

Thirty three chemicals across 9 different combustion-related particle samples were characterized and evaluated with their exposure patterns through WCCNA in an unsupervised manner. This analysis identified 4 different chemical groups (designated as modules to different colors) that represented clusters of co-modulated elemental, ionic, and carbonaceous components based on their relative abundances (Supplementary Table S6). Computational analysis demonstrated that fluoride, Cu, Co, Ni, and Li (brown module) were highly concentrated in the LIB smoke soot and PM, as compared to those in air pollution or biomass smoke PM previously reported (Fig. 5 and Supplementary Table S7). These increased concentrations were different from each other, with Co, Ni and Cu being in higher concentrations in the soot, while Li and fluoride had higher concentrations in the smoke PM. Unique chemical signatures of biomass smoke PM, urban ambient PM, residual oil fly ash, and diesel exhaust particles were also analyzed previously (Kim et al., 2022; Klein et al., 2026) and compared with chemical profiles of the LIB smoke soot and PM samples. Phosphate, and organic carbon (grey module) were highly abundant in biomass smoke samples (oak and eucalyptus smoke) while nitrate, chloride, Zn and Pb (blue module) were heavily concentrated in the urban air pollution sample (Ottawa). The residual oil fly ash contained higher sulfate, As, Mg, V, and Mo (turquoise module) than other smoke samples. Elemental carbon (grey module) was the highest relative abundance in the diesel exhaust particles. The WCCNA approach was also utilized to identify chemical modules (mixture effects) closely related to increasing lung toxicity responses (Supplementary Table S8). Note that the toxicity input values were averages derived from groups of 6 mice receiving the same treatment. While the brown module (LIB fire samples) was positively correlated with increased LDH and IL-6 levels in BALF, the blue (urban air pollution sample) and turquoise (oil fly ash) modules were identified as the chemical groups showing the largest number of positive associations with increased LDH, albumin, IL-6, MIP-2, and TNF-α levels, indicating that disruption of cell membrane integrity in the lung was more affected by the urban air pollution and oil fly ash samples than the LIB fire smoke samples in this study. The WCCNA approach was used to further identify which chemicals were most associated with the process of biological response to the combustion-related particle exposures (Fig. 5 and Supplementary Table S9–S10). The increase of the metals (Ni, Li, and Al, Ti) and ions (fluoride) in the LIB smoke soot and PM had a direct correlation with several toxicity outcomes observed in the sample cohort. Specifically, in the 24 h post exposure group there was a significant change in neutrophils (e.g., Ti: $p = 0.019$), IL-6 (e.g., Ti: $p = 0.033$ and Ni: $p = 0.034$), MIP-2 (e.g., Ti: $p = 0.003$ and Al: $p = 0.018$), protein (e.g., Ti: $p = 0.033$), NAG (e.g., Li: $p = 0.006$ and fluoride: $p = 0.004$), and LDH (e.g., Ti: $p = 0.029$) compared to the control cohort. Pb, Zn, and nitrate of the urban air pollution sample were found to be major contributors to the increased IL-6 (e.g., Pb: $p = 0.001$, Zn: $p = 0.001$, nitrate: $p = 0.001$), TNF-α (e.g., Pb: $p = 0.001$, Zn: $p = 0.001$, nitrate: $p = 0.001$) and MIP-2 (e.g., Pb: $p = 0.001$, Zn: $p = 0.001$, nitrate: $p = 0.001$) levels in the lungs. Mg, V, and Mo of the oil

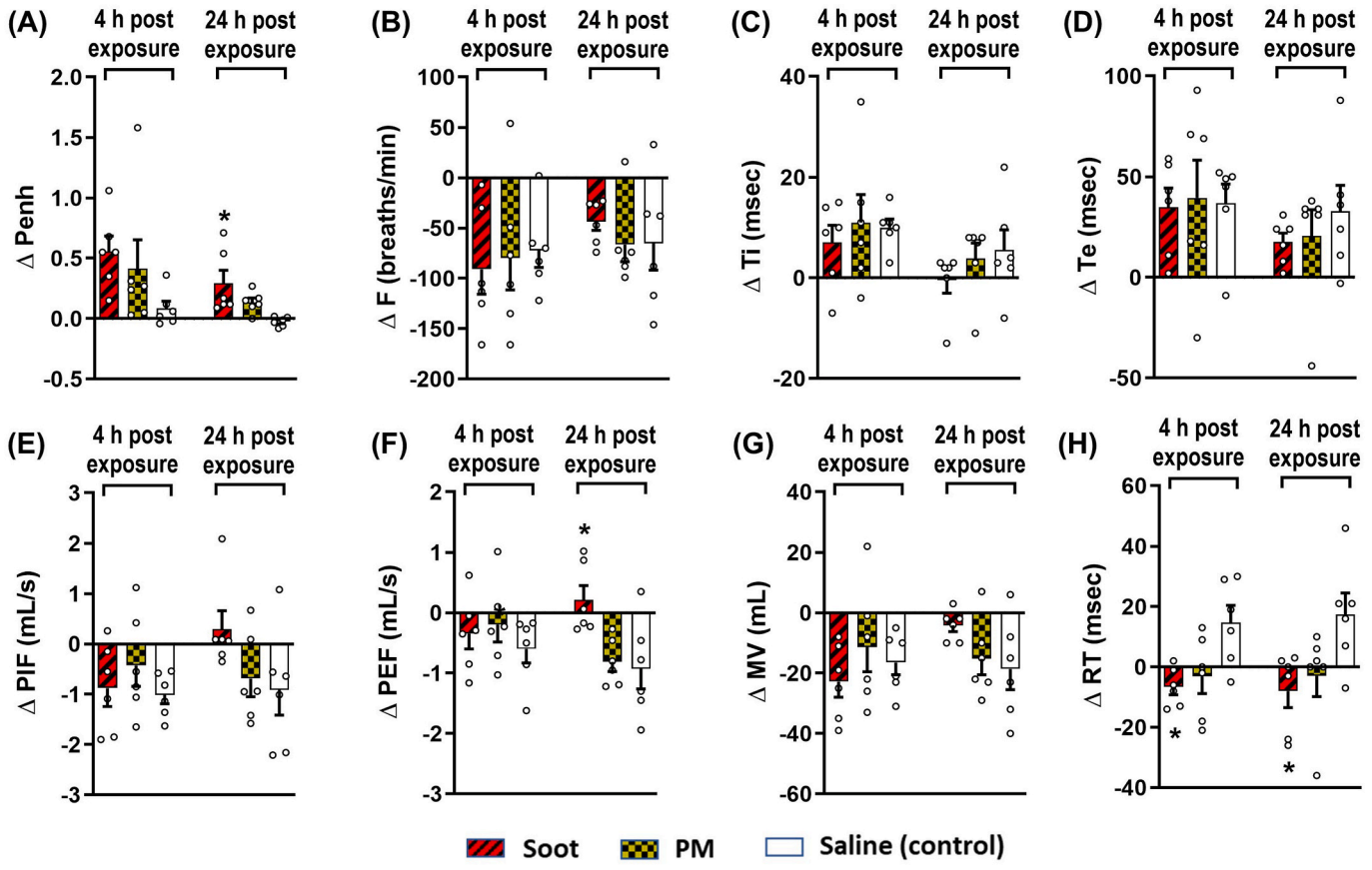


Fig. 4. Lung function of mice exposed to combustion particulate (soot or smoke PM) from Li-ion battery (LIB) fires. (A) Penh, (B) Breathing frequency (F), (C) Inspiratory time (Ti), (D) Expiratory time (Te), (E) Peak inspiratory flow (PIF), (F) Peak expiratory flow (PEF), (G) minute ventilation (MV), (H) Relaxation time (RT). Mice were exposed to the combustion particles (100 μg) by oropharyngeal aspiration and tested for breathing parameters 4 h and 24 h after exposure. Data are mean ± SEM obtained from 6 mice for each group. $^*p < 0.05$ compared with saline (control) group from the same time point (one-way ANOVA with post-hoc Dunnett's test).

fly ash sample were identified as the main chemicals that contributed significantly to the increased LDH level ($p < 0.001$). While organic carbon of the biomass smoke samples was significantly associated with the increased neutrophils ($p = 0.008$), IL-6 ($p = 0.001$), protein ($p = 0.007$), albumin ($p = 0.003$), LDH ($p = 0.001$), and GGT ($p = 0.004$) levels, elemental carbon of the diesel exhaust particles had no strong correlations with any biological responses.

4. Discussion

Chemical components of the smoke PM and soot samples collected from LIB fires varied; the soot contained higher concentrations of EC but did not show significant differences in other species (e.g., inorganic elements and ions). Specific chemical components (e.g., fluoride, Al, Fe, Ni, and Li) were significantly associated with pro-inflammatory lung responses and changes in breathing parameters in mice following exposures to the LIB fire samples compared to other air pollutant mixtures.

The largest percentage of identified chemicals in the samples was combined OC and EC, with EC making up 18.10% of the soot sample but only 5.00% of the PM sample. The OC/EC ratio that is used to characterize transformation of carbonaceous aerosols was calculated to be 1.0 for the soot and 2.6 for the smoke PM sample, suggesting that the soot contained more primary pollutants (e.g., EC) while more secondary pollutants (e.g., semi-VOCs) that are formed from chemical reactions were present in the smoke PM samples (Cao et al., 2006; Chow et al., 1996). The high EC percentage of the soot is indicative of a fuel that is not burning completely due to lack of oxygen. The lower level of EC in the PM sample is indicative of a more complete combustion process. The chemical makeup of the PM and the soot was similar, although mass percentages differed for some elements. The largest percentage of the samples were listed as unknown at 41.96% and 34.20% respectively. These portions are expected to be made up primarily of oxygen and hydrogen derivatives as metal oxide creation conditions will be met during combustion (Bolsaitis et al., 1987). Notably, it is well documented that the oxygen content in combustion samples can modulate lung inflammation and oxidative stress (Houseeiny et al., 2020). Within the framework of a nickel-cobalt-aluminum oxide ($LiNiCoAlO_2$ or NCA) LIB that was tested in the present study, the primary organic components include electrolytes, which are carbonate-based compounds, and separators, which are commonly fabricated from polymers such as polyethylene and polypropylene. During a fire, these compounds decompose, leading to the generation of substantial quantities of OC compounds (e.g., PAHs) and gases, which are subsequently released as hydrocarbons and organic matter.

The next largest identified group in the LIB fire samples, inorganic elements, was dominated by Li, Ni, Al, and Co which made up 87.62% and 94.03% of the total inorganic elements of the PM and soot, respectively. Similarly, these elements were predominant metals of smoke PM from electric vehicle fires compared to internal combustion engine vehicle fires, which can lead to more substantial mutagenic potencies (Kim et al., 2025). Some rodent model studies indicate that acute Li inhalation from combustion can cause laryngeal lesions, tracheal necrosis, and pneumonia (Greenspan et al., 1986; Rebar et al., 1986). Nanosized Ni has been demonstrated to cause oxidative stress and lung inflammation (Mo et al., 2019). The presence of Ni and Co in the lungs has been reported to cause lesions and the accumulation of

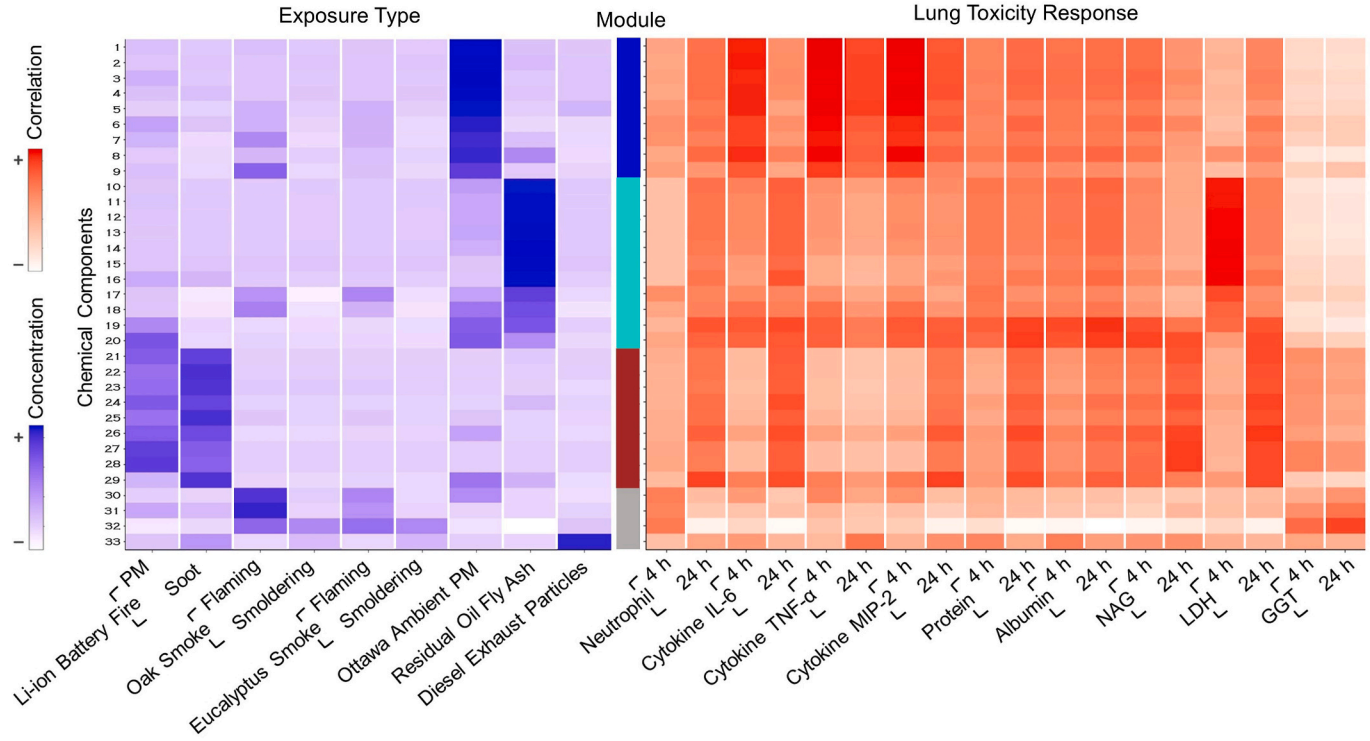


Fig. 5. Chemical profiles of various air pollutants (left) and their correlations with lung toxicity endpoints (right). The number represents individual chemical components, Blue module: (1) Ca, (2) Pb, (3) Nitrate, (4) Sn, (5) Zn, (6) Chloride, (7) K, (8) Sr, (9) Cd; Turquoise module: (10) Sulfate, (11) Mg, (12) Ce, (13) Nd, (14) La, (15) V, (16) Mo, (17) Cr, (18) Ba, (19) Fe, (20) Mn; Brown module: (21) Co, (22) Bromide, (23) Sb, (24) Ni, (25) Cu, (26) Al, (27) Li, (28) Fluoride, (29) Ti; Grey module: (30) Si, (31) Phosphate, (32) Organic carbon, (33) Elemental carbon. Values are represented as scaled values, normalized per study sample (left) or biological outcome type (right). For further details, see Supplementary Table S7–S10.

macrophages, a sign of inflammation (Johansson et al., 1992). There were several other inorganic elements after the main four (Ni, Li, Al, and Co) in both the soot and PM samples. The smoke PM sample had much more diverse concentrations of inorganic elements. Notably, some inorganic elements such as Fe (3.96% vs. 0.33%), Ca (3.61% vs. 0.84%), and Mg (0.92% vs. 0.18%) were much more abundant in smoke PM. This suggests that these elements are more likely to aerosolize compared to other elements found in the samples during LIB fires.

Fluoride, phosphate and chloride were found in both smoke PM and soot samples. This finding raises concerns about potential health risks from inhaling or being dermally exposed to these compounds. While these compounds were detected as particulate formation in this study, they are emitted in both gaseous and particulate forms from LIB fires (Bugryniec et al., 2024; Larsson et al., 2017). In addition, some gaseous forms (e.g., hydrogen fluoride and sulfur dioxide) easily interact with water to form ions that can then bind to their particulate forms. Thus, separating health effects of their particulate compounds from gaseous compounds would be challenging. Although particulate forms of fluoride, chloride, and sulfate are generally considered less toxic than their gaseous forms (AIHAJ, 1965; Grahame and Schlesinger, 2012; O'Donnell, 1995), they may increase health risks if they interact with their gaseous forms or other toxic chemicals. Fluoride can be converted to hydrogen fluoride (HF) during combustion, which can cause various health outcomes (National Research Council Committee, 2009). Chlorides, such as hydrogen chloride (HCl), and phosphates can be strong irritants when inhaled and may cause various other health effects. The smoke PM also contained sulfates and nitrates. Sulfates in smoke can become SO_2, which can cause oxidative stress, modify apoptosis triggers, and significantly raise the risk of chronic obstructive pulmonary disease (COPD) (Kheirouri et al., 2022; Zhou et al., 2024). Nitrates can also cause respiratory distress (Gupta et al., 2017). Note that the soot samples from other studies also contained the same metals and ions we observed in both PM and soot (Claassen et al., 2024b, Adanouj et al., 2023).

The biological and physiological effects associated with exposure to the LIB smoke PM and soot are outlined in Figs. 3 and 4. The most significant change in all the biomarkers examined was the neutrophil percentage increase in the 24 h exposure cohort. Cohorts exposed to both the smoke PM and soot sample exhibited comparatively similar high neutrophil influxes in the lungs. Our study used PM that would be considered PM10 (particles with an aerodynamic diameter of 10 μm or smaller), closely related with coarse PM. We compared the percentages of BALF neutrophils exposed to the LIB smoke samples with ambient samples that were sourced from combustion and urban air pollution previously studied (Fig. 6 and Supplementary Table S11). Interestingly, increased neutrophil percentages (adjusted for the control group) were closely associated with chemical components of the samples rather than the particle sizes, suggesting that the chemistry and emission source of PM could be of more potential health concerns than physical size alone. This is reasonable and supported by other studies (Damiati et al., 2025; Mirowsky et al., 2015; Seagrave et al., 2006). While understanding particle sizes is essential for health effects on the general population, identifying potent chemical constituents would be more targeted support to protect population at risk. In this study, the comparison of the neutrophil fractions in the lungs exposed to various air pollution samples (Fig. 6) showed that the toxicity of the smoke PM and soot was similar in magnitude to that of the coarse PM samples from an e-waste facility, and urban area (Cho et al., 2009; Kim et al., 2015) and also was comparable to the toxicity of the fine PM samples emitted from coal and oil combustions (Gilmour et al., 2004; Klein et al., 2026). While these coarse and fine PM samples derived from different emission sources they contained relatively high concentrations of various metals, suggesting that the presence of metals in the combustion byproducts from LIB fires could be key factors driving the toxicity outcomes.

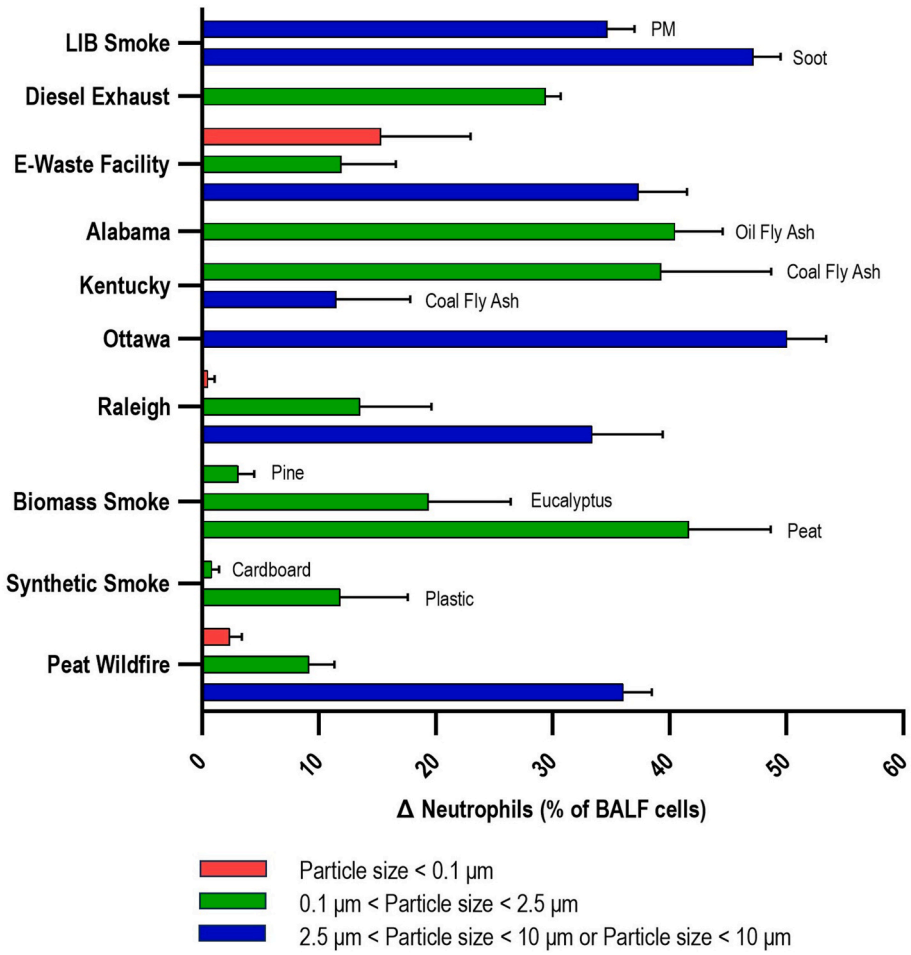


Fig. 6. Comparison of percentages of BALF neutrophils (adjusted for the control group) in the mouse lungs exposed to combustion particles emitted from LIB fires and air pollution samples from various sources, all at a concentration of 100 μg of sample. The percentages of neutrophils in BALF of the mouse lungs exposed to various air pollution samples are obtained from our previous studies: Diesel Exhaust (Klein et al., 2026), E-Waste Facility (Kim et al., 2015), Alabama, Kentucky (Gilmour et al., 2004), Ottawa, Raleigh (Cho et al., 2009), Synthetic Smoke (Kim et al., 2021), Biomass Smoke (Kim et al., 2018), Peat Wildfire (Kim et al., 2014).

Other significant changes that occurred in the 24 h cohorts exposed to both the smoke PM and soot were the increase of protein and IL-6 levels. These biomarkers indicate that there was both inflammation and loss of cell membrane integrity after acute exposure, but that it took several hours for them to become evident. While IL-6 levels largely increased in the 4 h cohorts, there was no significant increase in protein levels, suggesting that the acute exposure did not significantly influence the integrity of cell membrane at the early time point. Other biomarkers were only present in one exposure or the other, with MIP-2 levels being higher in both soot exposed cohorts, while albumin levels were higher in both 4 h and 24 h smoke PM exposed cohorts. This could indicate repression of effects caused by chemical interactions (Rager et al., 2021; Strongin et al., 2025). Notably, adverse biological effects (e.g., neutrophils, IL-6, MIP-2, protein, and albumin) were observed from the exposures to both the smoke PM and soot, while relatively minor but still significant physiological responses (e.g., Penh, PEF, RT, and EF50) changed only when exposed to the soot sample. This could be also explained by chemical interactions. There was a big difference in the chemical composition of two samples. The soot sample had 2 times higher levels of carbon substances with 3.6 times higher concentrations of elemental carbon. This is not surprising because soot particles are primarily composed of elemental carbon. Since elemental carbon has been widely recognized as a carrier of various toxic chemicals, the combination of elemental carbon and metals in the soot sample could worsen health risks (Cassee et al., 2013; Yamagami et al., 2019). The bioinformatics based approach provided a more in-depth understanding of these LIB fire repressors as well as substances that may cause potentially additive or greater-than-additive effects. Such methods have been used successfully in other studies where the total toxicity of an emission source is modified by interactions between individual toxicants (Rager et al., 2021). In this study, major chemical components of the LIB fire samples significantly correlated to increasing lung toxicity responses were compared with those of other combustion-related samples. Four different chemical modules (groups) were identified based on the major chemical components of each sample: the blue module (e.g., Pb, nitrate, and Zn), the turquoise module (e.g., Mg, V, and Mo), the brown module (e.g., Li, Ni, and Fe), and the grey module (e.g., OC and EC). Data-driven computational analysis showed (Fig. 5) that the increase of the metals (e.g., Ni, Al, Ti, and Li) and ions (e.g., fluoride) in the LIB soot and smoke PM (the brown module) had strong correlations with several toxicity outcomes (e.g., neutrophils, IL-6, MIP-2, protein, and LDH) observed in the sample cohort. Interestingly, while Pb, nitrate, and Zn in the urban air pollution samples (the blue module) were mainly associated with the increased IL-6, MIP-2 and TNF-α levels in the lungs, Mg, V, and Mo in the oil fly ash samples (the turquoise module) had significantly contributed to the increased LDH level, suggesting that inorganic elements may cause distinct toxicity responses based on how they interact with the lung cells. Similarly, carbonaceous compounds elicited different biological responses. EC in the diesel exhaust particles resulted in more muted responses compared to organic carbon in the biomass smoke samples. Notably, the LIB soot and diesel exhaust particles contained relatively high concentrations of EC, but they exhibited different toxicity

outcomes supporting the notion that EC may not be a major toxic component, but its toxicity could be enhanced by the presence of other components (e.g., metals) (Kong et al., 2025). Since exposure likely occurs by inhalation of a mixture of chemicals rather than single chemical, it is critical to know mixture interactions. Although the WCCNA approach identified correlation between each chemical and lung toxicity responses, it was also used to evaluate the toxicity responses if individual chemicals act differently in the presence of additional chemicals (Supplementary Table S8). This mixture-based approach demonstrated that chemical mixtures in the LIB fire samples exhibited moderate correlations with lung toxicity responses, while chemical mixtures in the urban air pollution and oil fly ash samples were still strongly correlated with inflammatory responses. This suggests that chemical mixtures can produce joint effects that differ substantially from those of individual substances (Domingo and Nadal, 2026). While additional work in mechanistic toxicology is necessary, this information could be used to identify hazardous chemical sources that were aerosolized from LIB fires, improving both protection from and treatment of toxic emissions.

There are several contamination and toxicity studies on the residue from LIB fires. Many of the residues include Li, oxides of varying metals depending on the cathode material, and particulate fluorides. While we only focused on LIBs with a makeup of $LiNiCoAlO_2$, the literature focused on other battery chemistries that were similar to ours. This would indicate that the toxicity outcomes our study observed would closely model the toxicity outcomes from fires involving LIBs with different constructions. Specifically, lung toxicity of lithium cobalt oxide ($LiCoO_2$) and nickel manganese cobalt (NMC) which are widely used cathode materials of LIB, have been evaluated using both in vitro and in vivo models, demonstrating that lung inflammatory responses are associated with metal ions released from the cathode material (Sironval et al., 2019, 2020; Wang et al., 2025; Zhang et al., 2026). Interestingly, a recent study showed that manganese-based cathodes produced more gas and were more toxic than manganese-free cathodes (e.g., lithium iron phosphate), suggesting that there could be differences in lung toxicity depending on the LIB cathode chemistry (Meister et al., 2025). While there are studies evaluating chemical profiles of LIB fire emissions, there are very few toxicity studies from LIB fire smoke exposures. In addition to the lung toxicity depending on battery chemistry, there is evidence that the amount of PM generated, as well as the gas emissions, can change depending on charge levels (Claassen et al., 2024b; Peng et al., 2020; Premnath et al., 2025; Sun et al., 2016), further research is needed to investigate adverse health effects of smoke emissions from LIB burns at different states of charge. Few other studies looked at ambient PM and primarily focused on gas emissions and soot (Hynynen et al., 2023; Kwon et al., 2024; Ribière et al., 2012; Zhang et al., 2019), demonstrating that CO, CO_2, HF, HCl, and hydrogen bromide (HBr) were present in varying concentrations. Although we did not measure gases, the compounds and anions we detected suggest that these gases were likely produced from the LIB fires tested in the present study.

Our study has several limitations that should be considered when interpreting our findings; (1) we studied one type of LIB construction and chemistry (vs. multiple types of LIBs). (2) we focused on acute exposure (vs. long-term exposure). (3), we evaluated exposure to particles (vs. whole smoke). (4) we did not fully characterize organic carbon (e.g., PAHs). The chemical makeup of LIB anodes can vary widely; however, the more notable elements of concern, such as Ni, Li, Co, and Fe are present in some amounts in the LIB that we sampled. As long as the major chemical components are similar, it may not be necessary to test all different types of LIBs, and the use of the computational approach addressed here could help determine the correlation between the element concentrations and the health effects observed. Regarding the acute exposure method, this study represents potential exposure conditions for emergency first responders (e.g., firefighters and paramedics) during LIB fire events. There are often spikes of PM generation at the beginning of LIB fires, lasting for several seconds to minutes, which represents the most likely cases of exposure (specifically for firefighters and other first responders) (Claassen et al., 2024a; Premnath et al., 2025). However, additional studies for long-term and/or repeated short-term health risks of firefighters and the general public are warranted to understand how chronic exposure to LIB fire smoke can cause detrimental effects to health and whether they are different from health effects of acute exposure. Our use of particles isolated from the LIB fire smoke demonstrates lung inflammatory responses associated with chemicals that can be easily delivered by the instillation exposure method used here. However, it is also necessary to use a whole smoke exposure method to investigate inflammatory responses of hazardous gas components (e.g., VOCs and gas phase PAHs). Moreover, there are likely other hazardous chemicals (e.g., PAHs) associated with organic carbon that are not characterized in this study. Future research should utilize a whole smoke inhalation exposure method and require more careful consideration of organic carbon species, which would provide a better understanding of how lung toxicity data from LIB fire smoke can be extrapolated to humans from animal studies.

5. Conclusion

This study demonstrated that combustion byproducts (smoke PM and soot) from LIB fires contain hazardous metals and particulate fluoride and that acute exposure to LIB soot and smoke PM can cause abnormal breathing patterns and lung inflammation. The toxicity of the LIB soot and smoke PM was similar to some of the most highly polluted samples that have been previously studied. Moreover, the data-driven computational analysis showed that fluoride, Al, Fe, Ni, and Li from both samples were highly associated with the lung toxicity responses. To the best of our knowledge, this is the first study to determine chemical components of particulate-phase combustion byproducts of LIB fires and their biological and physiological responses in the lungs. Identifying specific chemicals is useful to fill the knowledge gap of the toxicity of LIB fire smoke emissions. This information may be used to develop effective exposure mitigation strategies and enable more targeted treatment of exposed populations during LIB fires and post-fire cleanup/restoration activities.

CRediT authorship contribution statement

Adam Nored: Writing – original draft, Formal analysis, Data curation. **Gavin P. Horn:** Resources, Methodology, Investigation. **Richard M. Kesler:** Writing – review & editing, Resources, Methodology, Investigation. **Adam Barowy:** Resources, Methodology, Investigation. **Alex Schraiber:** Resources, Methodology, Investigation. **Benjamin Gaudet:** Resources, Methodology, Investigation. **Alexander C. Mayer:** Writing – review & editing, Resources, Methodology, Investigation. **Kenneth W. Fent:** Resources, Methodology, Investigation. **Micah Niemeier-Walsh:** Resources, Methodology, Investigation. **David Naiman:** Methodology, Investigation. **Logan M. Klein:** Methodology, Investigation. **Mette Schladweiler:** Methodology, Investigation. **Wanda Williams:** Methodology, Investigation. **Rachel Grindstaff:** Methodology, Investigation. **Kasey Kovalcik:** Methodology, Investigation. **Joseph Patrick Pancras:** Methodology, Investigation. **Andrew F.M. Johnstone:** Methodology, Investigation. **Julia E. Rager:** Software, Conceptualization. **Stephen H. Gavett:** Writing – review & editing, Investigation. **M. Ian Gilmour:** Writing – review & editing, Supervision, Conceptualization. **Yong Ho Kim:** Writing – review & editing, Supervision, Project administration, Methodology, Formal analysis, Data curation, Conceptualization.

Ethics declaration

This study was conducted in accordance with the ARRIVE (Animal Research: Reporting of In Vivo Experiments) guidelines. This study was approved by the EPA Institutional Animal Care and Use Committee.

(Approval No. 27-04-001)

Funding

Part of this work was funded by the NIOSH Nanotechnology Research Center (NTRC).

Declaration of competing interest

The authors declare the following financial interests/personal relationships which may be considered as potential competing interests: Alexander C. Mayer reports financial support was provided by NIOSH Nanotechnology Research Center. If there are other authors, they declare that they have no known competing financial interests or personal relationships that could have appeared to influence the work reported in this paper.

Acknowledgements

The research described in this manuscript has been reviewed by the Center for Public Health & Environmental Assessment, U.S. EPA, and approved for publication. Approval does not signify that contents necessarily reflect the views and policies of the agency, nor does the mention of trade names or commercial products constitute endorsement or recommendation for use. The findings and conclusions in this paper are those of the authors and do not necessarily represent the official position of the National Institute for Occupational Safety and Health (NIOSH) or Centers for Disease Control and Prevention (CDC). Mention of any company or product does not constitute endorsement by NIOSH or CDC.

Appendix A. Supplementary data

Supplementary data to this article can be found online at https://doi.org/10.1016/j.envres.2026.126023.

Data availability

Data will be made available on request.

References

AIHAJ, 1965. Fluoride-bearing dusts and fumes (inorganic). Am. Ind. Hyg. Assoc. J. 26, 426–430.

Adanouj, I., Napolitano, E., Sommariva, M., Enzo, S., Lebedeva, N., 2023. Characterisation of smoke particles from lithium-ion battery fire: morphology, size and composition. Meet. Abstr., MA2023-02 431.

Bharadwaj, S., Levers, A., Yeung, L., Hutchinson, A., Magrath, A., 2024. Street safety in the era of micromobility. New York City Comptroller. https://comptroller.nyc.gov/reports/street-safety-in-the-era-of-micromobility/. New York, NY.

Bolsaitis, P., McCarthy, J., Mohiuddin, G., Elliott, J., 1987. Formation of metal oxide aerosols for conditions of high supersaturation. Aerosol. Sci. Technol. 6, 225–246.

Bugryniec, P.J., Resendiz, E.G., Nwophoke, S.M., Khanna, S., James, C., Brown, S.F., 2024. Review of gas emissions from lithium-ion battery thermal runaway failure — considering toxic and flammable compounds. J. Energy Storage 87, 111288.

Cao, J.J., Lee, S.C., Ho, K.F., Fung, K., Chow, J.C., Watson, J.G., 2006. Characterization of roadside fine particulate carbon and its eight fractions in Hong Kong. Aerosol Air Qual. Res. 6, 106–122.

Cassee, F.R., Héroux, M.E., Gerlofs-Nijland, M.E., Kelly, F.J., 2013. Particulate matter beyond mass: recent health evidence on the role of fractions, chemical constituents and sources of emission. Inhal. Toxicol. 25, 802–812.

Cho, S.-H., Tong, H., McGee, J.K., Baldauf, R.W., Krantz, Q.T., Gilmour, M.I., 2009. Comparative toxicity of size-fractionated airborne particulate matter collected at different distances from an urban highway. Environ. Health Perspect. 117, 1682–1689.

Chow, J.C., Watson, J.G., Lu, Z., Lowenthal, D.H., Frazier, C.A., Solomon, P.A., et al., 1996. Descriptive analysis of pm2.5 and pm10 at regionally representative locations during sjvaqs/auspex. Atmos. Environ. 30, 2079–2112.

Claassen, M., Bingham, B., Chow, J.C., Watson, J.G., Chu, P., Wang, Y., et al., 2024a. Characterization of lithium-ion battery fire emissions—part 2: particle size distributions and emission factors. Batteries 10, 366.

Claassen, M., Bingham, B., Chow, J.C., Watson, J.G., Wang, Y., Wang, X., 2024b. Characterization of lithium-ion battery fire emissions—part 1: chemical composition of fine particles (pm2. 5). Batteries 10, 301.

Damiati, S., AlMashrea, B.A., Rabiei, N., Sujatha, A.P., Sabir, D.K., Alhosani, M., et al., 2025. Aerosol pollutants and health: role of size and chemical composition. Public Health Chall 4, e70134.

Domingo, J.L., Nadal, M., 2026. Mixture toxicity in human health: integrating one health, exposomics, and modern risk assessment strategies. Chem. Res. Toxicol. 39, 738–751.

Feng, X., Ouyang, M., Liu, X., Lu, L., Xia, Y., He, X., 2018. Thermal runaway mechanism of lithium ion battery for electric vehicles: a review. Energy Storage Mater. 10, 246–267.

Foster, W.M., Walters, D.M., Longphre, M., Macri, K., Miller, L.M., 2001. Methodology for the measurement of mucociliary function in the mouse by scintigraphy. J. Appl. Physiol. 90, 1111–1117, 1985.

Gilmour, M.I., O'Connor, S., Dick, C.A., Miller, C.A., Linak, W.P., 2004. Differential pulmonary inflammation and in vitro cytotoxicity of size-fractionated fly ash particles from pulverized coal combustion. J. Air Waste Manag. Assoc. 54, 286–295.

Grahame, T., Schlesinger, R., 2012. Is ambient pm2.5 sulfate harmful? Environ. Health Perspect. 120, A454 author reply A454-455.

Greenspan, B.J., Allen, M.D., Rebar, A.H., Boecker, B.B., 1986. Inhalation toxicity of lithium combustion aerosols in rats. J. Toxicol. Environ. Health, Part A Current Issues 18, 627–637.

Gupta, S., Gupta, A., Gupta, R., 2017. Pathophysiology of nitrate toxicity in humans in view of the changing trends of the global nitrogen cycle with special reference to India. In: The Indian Nitrogen Assessment. Elsevier, pp. 459–468.

Housseiny, H.A., Singh, M., Emile, S., Nicoleau, M., Wal, R.L.V., Silveyra, P., 2020. Identification of toxicity parameters associated with combustion produced soot surface chemistry and particle structure by in vitro assays. Biomedicines 8, 345.

Hynynen, J., Willstrand, O., Blomqvist, P., Andersson, P., 2023. Analysis of combustion gases from large-scale electric vehicle fire tests. Fire Saf. J. 139, 103829.

Jo, M.S., Kim, H.P., Kim, B.W., Pleus, R.C., Faustman, E.M., Yu, I.J., 2024. Exposure assessment study on lithium-ion battery fire in explosion test room in battery testing facility. Saf. Health Work 15, 114–117.

Johansson, A., Curstedt, T., Jarstrand, C., Camner, P., 1992. Alveolar macrophages and lung lesions after combined exposure to nickel, cobalt, and trivalent chromium. Environ. Health Perspect. 97, 215–219.

Kheirouri, S., Shanehbandi, D., Khordadmehr, M., Alizadeh, M., Eskandari Vaezi, F., Musapour Sultan Abad, R., et al., 2022. Effects of sulfur dioxide, ozone, and ambient air pollution on lung histopathology, oxidative-stress biomarkers, and apoptosis-related gene expressions in rats. Exp. Lung Res. 48, 137–148.

Kim, Y.H., Nored, A., Horn, G.P., Kesler, R.M., Barowy, A., Schraiber, A., et al., 2025. Chemical components of electric vehicle and internal combustion engine vehicle fire smoke and their mutagenic effects. Environ. Sci. Pollut. Res. Int. 32, 26629–26639.

Kim, Y.H., Rager, J.E., Jaspers, I., Gilmour, M.I., 2022. Computational approach to link chemicals in anthropogenic smoke particulate matter with toxicity. Chem. Res. Toxicol. 35, 2210–2213.

Kim, Y.H., Tong, H., Daniels, M., Boykin, E., Krantz, Q.T., McGee, J., et al., 2014. Cardiopulmonary toxicity of peat wildfire particulate matter and the predictive utility of precision cut lung slices. Part. Fibre Toxicol. 11, 1–17.

Kim, Y.H., Warren, S.H., Kooter, I., Williams, W.C., George, I.J., Vance, S.A., et al., 2021. Chemistry, lung toxicity and mutagenicity of burn pit smoke-related particulate matter. Part. Fibre Toxicol. 18, 45.

Kim, Y.H., Warren, S.H., Krantz, Q.T., King, C., Jaskot, R., Preston, W.T., et al., 2018. Mutagenicity and lung toxicity of smoldering vs. flaming emissions from various biomass fuels: implications for health effects from wildland fires. Environ. Health Perspect. 126, 017011.

Kim, Y.H., Wyrzykowska-Ceradini, B., Touati, A., Krantz, Q.T., Dye, J.A., Linak, W.P., et al., 2015. Characterization of size-fractionated airborne particles inside an electronic waste recycling facility and acute toxicity testing in mice. Environ. Sci. Technol. 49, 11543–11550.

Klein, L.M., Gavett, S.H., Pancras, J.P., Williams, W.C., Nored, A., Gilmour, M.I., et al., 2026. Chemical clustering analysis of ambient and emission source particulate matter reveals compositional determinants of pulmonary toxicity responses. Chem. Res. Toxicol. 39, 319–328.

Kong, Y., Wang, Q., Li, L., Zhang, Y., Tian, J., Ma, N., et al., 2025. Chemical composition and mixing state of elemental carbon-containing particles from solid fuel combustion. npj Clim. Atmos. Sci. 8, 202.

Kwon, B., Schraiber, A., Jeevarajan, J.A., 2024. Evaluating fire and smoke risks with lithium-ion cells, modules, and batteries. ACS Energy Lett. 9, 5319–5328.

Larsson, F., Andersson, P., Blomqvist, P., Mellander, B.E., 2017. Toxic fluoride gas emissions from lithium-ion battery fires. Sci. Rep. 7, 10018.

Lundblad, L.K., 2012. Issues determining direct airways hyperresponsiveness in mice. Front. Physiol. 3, 408.

Lundblad, L.K., Irvin, C.G., Adler, A., Bates, J.H., 2002. A reevaluation of the validity of unrestrained plethysmography in mice. J. Appl. Physiol. 93, 1198–1207, 1985.

Meister, M., Sharma, S., He, X., Chepaitis, P.S., Waddey, T., Wilson, M., et al., 2025. Evaluating inhalation risks and toxicological impacts of lithium-ion battery thermal runaway emissions. Environ. Int. 199, 109466.

Mirowsky, J.E., Jin, L., Thurston, G., Lighthall, D., Tyner, T., Horton, L., et al., 2015. In vitro and in vivo toxicity of urban and rural particulate matter from california. Atmos. Environ. 103, 256–262, 1994.

Mitzner, W., Tankersley, C., 1998. Noninvasive measurement of airway responsiveness in allergic mice using barometric plethysmography. Am. J. Respir. Crit. Care Med. 158, 340–341.

Mo, Y., Jiang, M., Zhang, Y., Wan, R., Li, J., Zhong, C.-J., et al., 2019. Comparative mouse lung injury by nickel nanoparticles with differential surface modification. J. Nanobiotechnol. 17, 1–18.
NACTO, 2023. Shared micromobility report in the u.S. and Canada: 2023. https://nacto.org/publication/shared-micromobility-report-2023/.
National Research Council Committee, 2009. Emergency and Continuous Exposure Guidance Levels for Selected Submarine Contaminants; Volume 3. National Academies Press, Washington (DC), 4. Hydrogen fluoride.
O'Donnell, T.V., 1995. Asthma and respiratory problems–a review. Sci. Total Environ. 163, 137–145.
Ouf, F.X., Bourrous, S., Fauvel, S., Kort, A., Lintis, L., Nuvoli, J., et al., 2019. True density of combustion emitted particles: a comparison of results highlighting the influence of the organic contents. J. Aerosol Sci. 134, 1–13.
Palma, D., Ubaldi, S., Quinterno, M., Gentile, P., Mazzaro, M., Russo, P., 2024. Experimental & theoretical study on the solid, liquid and gaseous residues after fire extinction of lithium-ion batteries. Chem. Eng. Trans. 111, 475–480.
Peng, Y., Yang, L., Ju, X., Liao, B., Ye, K., Li, L., et al., 2020. A comprehensive investigation on the thermal and toxic hazards of large format lithium-ion batteries with lifepo4 cathode. J. Hazard Mater. 381, 120916.
Premnath, V., Parhizi, M., Niemiec, N., Smith, I., Jeevarajan, J., 2025. Characterization of particulate emissions from thermal runaway of lithium-ion cells. J. Electrochem. Energy Convers. Storage 22.
Rager, J.E., Clark, J., Eaves, L.A., Avula, V., Niehoff, N.M., Kim, Y.H., et al., 2021. Mixtures modeling identifies chemical inducers versus repressors of toxicity associated with wildfire smoke. Sci. Total Environ. 775, 145759.
Rebar, A., Greenspan, B., Allen, M., 1986. Acute inhalation toxicopathology of lithium combustion aerosols in rats. Toxicol. Sci. 7, 58–67.
Ribière, P., Grugeon, S., Morcrette, M., Boyanov, S., Laruelle, S., Marlair, G., 2012. Investigation on the fire-induced hazards of li-ion battery cells by fire calorimetry. Energy Environ. Sci. 5, 5271–5280.
Roman, J., 2025. Battery Safety; Incremental Learning. NFPA Journal, pp. 30–36.
Said, A.O., Lee, C., Stoliarov, S.I., Marshall, A.W., 2019. Comprehensive analysis of dynamics and hazards associated with cascading failure in 18650 lithium ion cell arrays. Appl. Energy 248, 415–428.
Seagrave, J., McDonald, J.D., Bedrick, E., Edgerton, E.S., Gigliotti, A.P., Jansen, J.J., et al., 2006. Lung toxicity of ambient particulate matter from southeastern u.S. sites with different contributing sources: relationships between composition and effects. Environ. Health Perspect. 114, 1387–1393.
Sironval, V., Palmai-Pallag, M., Vanbever, R., Huaux, F., Mejia, J., Lucas, S., et al., 2019. Hif-1α is a key mediator of the lung inflammatory potential of lithium-ion battery particles. Part. Fibre Toxicol. 16, 35.
Sironval, V., Scagliarini, V., Murugadoss, S., Tomatis, M., Yakoub, Y., Turci, F., et al., 2020. Licoo(2) particles used in li-ion batteries induce primary mutagenicity in lung cells via their capacity to generate hydroxyl radicals. Part. Fibre Toxicol. 17, 6.
Strongin, R.M., Sharma, E., Erythropel, H.C., Kassem, N.O., Noël, A., Peyton, D., et al., 2025. Chemical and Physiological Interactions Between e-liquid Constituents: Cause for Concern? BMJ Publishing Group Ltd.
Sturm, P., Fößleitner, P., Fruhwirt, D., Galler, R., Wenighofer, R., Heindl, S.F., et al., 2022. Fire tests with lithium-ion battery electric vehicles in road tunnels. Fire Saf. J. 134, 103695.
Sun, J., Li, J., Zhou, T., Yang, K., Wei, S., Tang, N., et al., 2016. Toxicity, a serious concern of thermal runaway from commercial li-ion battery. Nano Energy 27, 313–319.
Sun, J., Mao, B., Wang, Q., 2021. Progress on the research of fire behavior and fire protection of lithium ion battery. Fire Saf. J. 120, 103119.
Tran, M.-K., Mevawalla, A., Aziz, A., Panchal, S., Xie, Y., Fowler, M., 2022. A review of lithium-ion battery thermal runaway modeling and diagnosis approaches. Processes 10, 1192.
UL 2596, 2023. Test method for thermal and mechanical performance of battery enclosure materials. UL Standard & Engagement.
UL White Paper, 2025. The Impact of E-mobility Battery Fires in NYC. UL Standards & Engagement. https://ulse.org/insight/data-insights-impact-e-mobility-battery-fires-nyc/.
US Department of Energy. Active transportation and micromobility. (Office of Critical Minerals and Energy Innovation). https://afdc.energy.gov/conserve/active-transportation.
Wang, J., Fang, X., Wu, R., Liu, Z., Wang, G., Hu, Y., et al., 2025. Airway exposure to lithium nickel manganese cobalt oxide particles induces alterations in lung microenvironment and potential kidney and liver damage in mice. Toxicology 511, 154036.
Wang, Q., Mao, B., Stoliarov, S.I., Sun, J., 2019. A review of lithium ion battery failure mechanisms and fire prevention strategies. Prog. Energy Combust. Sci. 73, 95–131.
Weibel, E.R., 1973. Morphological basis of alveolar-capillary gas exchange. Physiol. Rev. 53, 419–495.
Yamagami, M., Ikemori, F., Nakashima, H., Hisatsune, K., Osada, K., 2019. Decreasing trend of elemental carbon concentration with changes in major sources at mega city Nagoya, central Japan. Atmos. Environ. 199, 155–163.
Zhang, X., Ye, X., Sun, Q., Liu, Q., Deng, F., Gu, W., et al., 2026. Respiratory exposure to lithium nickel manganese cobalt oxide particles: evidence for toxicity and disruption of metal homeostasis in mice. Environ. Health (Wash) 4, 618–629.
Zhang, Y., Wang, H., Li, W., Li, C., 2019. Quantitative identification of emissions from abused prismatic ni-rich lithium-ion batteries. eTransportation 2, 100031.
Zhou, X., Wang, X., Shen, Q., Ma, J., Cai, X., Liu, H., et al., 2024. Short-term exposure to sulfur dioxide and the occurrence of chronic obstructive pulmonary disease: an updated systematic review and meta-analysis based on risk of bias and certainty of evidence. Ecotoxicol. Environ. Saf. 284, 116888.